

Modelling phase changes in the potassium titanyl phosphate system

Leslie Glasser*[†] and C. Richard A. Catlow[‡]

Centre for Molecular Design, Dept. of Chemistry, University of the Witwatersrand, P O Wits 2050, South Africa and Royal Institution of Great Britain, 21 Albemarle Street, London, UK W1X 4BS

Potassium titanyl phosphate (KTiOPO₄, KTP) is the principal member of a group of isomorphous compounds, some of which have important non-linear optical properties. These structures have the acentric space group symmetry *Pna*2₁ and are ferroelectric. KTP itself undergoes a first-order, displacive isosymmetric phase change at 5.8 GPa at ambient temperature, as well as a second-order, displacive, order–disorder change to a paraelectric phase, with space group *Pnan*, under ambient pressure at 934 °C. Eight of these materials have been modelled using the static lattice modelling techniques in the GULP code. The materials modelled are: potassium, thallium and rubidium titanyl phosphates; potassium stannyl phosphate; potassium vanadyl phosphate; and potassium, rubidium and caesium titanyl arsenates. The modelling of the effects of pressure (based on the ambient pressure structures only) reproduces the isosymmetric phase change in KTP, and predicts similar pressure-driven phase changes for seven of the eight structures; only CsTiOAsO₄ fails to demonstrate this phase change. Certain of the high pressure structures modelled are rotationally twinned relative to their ambient pressure progenitor structures, in a manner in accord with suggestions in the literature. It did not prove possible to model the temperature-driven phase change using a static, ordered model; this problem is ascribed to disorder in the cation positions in the high-temperature phase.

The potassium titanyl phosphate (KTP) system¹ (see Table 1 for a list of the abbreviations used for these materials) consists of some one hundred isomorphous compounds of general formula AMOXO₄, of which some members (in particular KTP itself and KTA) have important non-linear optical properties, making them suitable as second-harmonic generators for Nd:YAG lasers. They also have great mechanical and thermal stability, which renders them reliable in fabrication and use.

The great chemical versatility of the system stems from the facts that there are two independent formula units per asymmetric unit, and that each of the ionic species may be replaced without structural disruption. Thus, the potassium ion (which may be regarded as a guest in a TiOPO₄ host framework) can be replaced by Na⁺, Ti⁴⁺, NH₄⁺, Ag⁺, Cs⁺ and Rb⁺, by direct synthesis, by ion exchange, or even by small-molecule gaseous exchange. In the framework, the Ti^{IV} ion may be replaced by other tetravalent ions such as V, Zr, Ge, Sb, Ta and Sn, or the mixed ions Fe^{III}/Nb^V, while the P^V ion can be substituted in various proportions by As, Si or Ge. It is even possible, in a charge balancing process, to replace oxide ions by fluoride and hydroxide ions when trivalent ions (such as Ga) replace the tetravalent Ti ions, as in, for example, KGaPO₄F_{0.7}(OH)_{0.3}.

The ambient crystal structure is orthorhombic, in the acentric, ferroelectric, space group *Pna*2₁; this acentricity permits the observed second-harmonic generation, which is necessarily absent in a centric space group. At elevated temperatures (934 °C for KTP, but only 581 °C for TTP), the structures undergo a second-order displacive phase transition² to the centric, paraelectric space group *Pnan*; indeed, the low-temperature phase already has a *Pnan* pseudo-symmetry.³ The effect of pressure on the room-temperature structure is rather more unexpected since there is a first-order displacive but isosymmetric (*i.e.*, no change in space group) phase change at about 6 GPa in those structures which have been studied under pressure, namely KTP^{4–9} and TTP⁹ (with the possibility of a further phase change at about 8 GPa in TTP).

The framework in the crystal structure of KTP under ambient conditions^{10,11} consists of distorted TiO₆ octahedra

in chains, linked by tetrahedral PO₄ bridges (Fig. 1). The K⁺ guest ions lie within open channels in the framework and can move most readily along the crystallographic *c* direction, leading to a strongly anisotropic electrical conductivity.¹ Adjacent to each of the two K⁺ sites there is a ‘hole’ site,¹² which is involved in the twinning process in the crystals, and which provides a possibility of some disorder in the ion positions by motion between the ion and hole sites. In the high-temperature structure, the ion and hole sites coalesce into symmetry-determined positions.^{3,10} The temperature- and pressure-driven phase changes retain the framework structure of KTP. Under pressure, the K cages diminish in volume slightly by the buckling of the chains of TiO₆ octahedra and PO₄ tetrahedra,^{3,10} while the K⁺ ions move towards their ‘ideal’ *Pnan* positions (Fig. 2).

Given this large chemical versatility within a rather limited, but intriguing, structural environment, it is clear that there is considerable value in (and scope for) computational studies because a successful modelling of the structures and their phase changes will permit ready examination of a wide range of chemical modifications under experimentally accessible conditions (and even such inaccessible conditions as negative pressures), which may provide interesting and useful predictive patterns for further experimental studies. No such study on this system has previously been reported.

Potential model

The structures have here been modelled using standard static lattice modelling techniques, employing the GULP program¹³

Table 1 Abbreviations used for materials in this study

abbreviation	name	empirical formula
KTP	potassium titanyl phosphate	KTiOPO ₄
TTP	thallium titanyl phosphate	TlTiOPO ₄
RTP	rubidium titanyl phosphate	RbTiOPO ₄
KSP	potassium stannyl phosphate	KSnOPO ₄
KVP	potassium vanadyl phosphate	KVOPO ₄
KTA	potassium titanyl arsenate	KTiOAsO ₄
RTA	rubidium titanyl arsenate	RbTiOAsO ₄
CTA	caesium titanyl arsenate	CsTiOAsO ₄

[†] E-mail: glasser@aurum.chem.wits.ac.za

[‡] E-mail: richard@ri.ac.uk

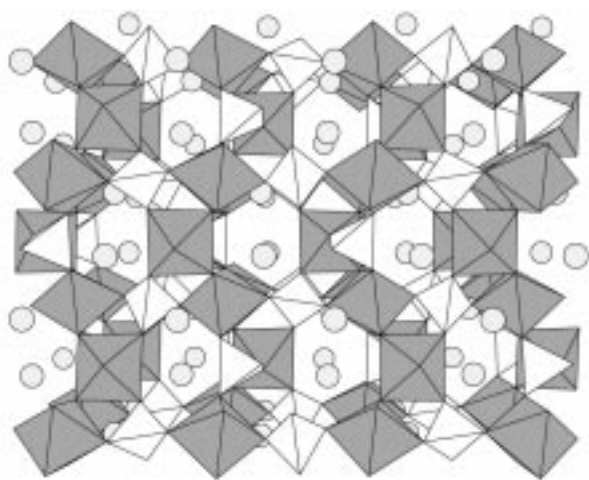


Fig. 1 Perspective view of the structure of KTP under ambient conditions.³ Octahedra represent TiO_6 , tetrahedra are PO_4 , spheres are K^+ . The orthogonal crystallographic axes are directed as follows: a to the left; c vertical in the plane of the paper; and b normal to the paper. The structural diagrams were prepared with the aid of ATOMS ver. 4.0 by E. Dowty (Shape Software, 1997).

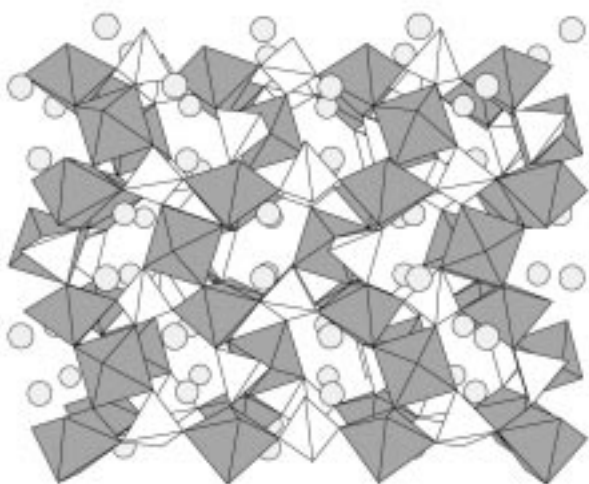


Fig. 2 Perspective view of the structure of KTP at 8.2 GPa.⁸ The crystallographic axes are directed as in Fig. 1.

(which has a variety of built-in potential functions such as the Buckingham exp-6 potential, the Morse potential, and many others). The crystals are described using the Born model, where formal integral charges are associated with each species (K^+ , Ti^{4+} , P^{5+} , O^{2-} , etc.) which also interact with the oxide ion shells by a Buckingham exp-6 potential; the oxide ion is modelled using an $\text{O}^{2-}(\text{shell})\text{--O}^{2-}(\text{shell})$ potential with charge distributed between core and shell;¹⁴ the P–O potential is taken from studies on aluminophosphates;¹⁵ the K–O potential is derived from a study of complex oxides;¹⁶ and the Ti–O potential comes from studies on the Ti–O oxide system.¹⁷ These potentials and their associated parameters, before and after fitting to the relevant structures, are listed in Table 2. As is usual in studies of this kind, no non-coulombic cation–cation interactions have been taken into account since their values are negligibly small.¹⁴ The K–O and Ti–O (and, if required, the P–O) potential parameters were fitted to the KTP structures, but the other parameters were retained at their input values. For a few of the materials (KTP, TTP and RTP), elastic constants have been determined by Brillouin scattering methods.¹⁸ Where known, these values were used in an additional parameter fitting process in GULP: once with

the structure alone as the observable; and again with both the structure and the elastic constants as observables.

It is important in fitting the potential parameters to the structures to ensure that the structures relax with little distortion under the fixed space group symmetry. To this end we use the ‘fit relax constant_pressure’ set of options in the GULP code, rather than the more conventional ‘fit constant_pressure’ set. In the latter case, the forces on the species (the energy derivatives) are minimised but this does not always lead to a usable set of parameters while, with the former choice, the structural displacements of the ions and their shells on relaxation from their crystallographic positions are minimised, which is more directly what is sought. However, the ‘relax’ option also leads to an order of magnitude increase in computer time, and requires that the initial values for the parameters are already good, otherwise the fitting may fail.

The procedure used for fitting of parameters to related structures (KTA, KSP, TTP, RTP, KVP, RTA and CTA) was to commence with the newly established parameters for KTP (or of a more-closely related structure), and then proceed through cycles of fitting to generate optimal parameters for the new material. In each case, the structure was subsequently relaxed, employing the newly fitted parameters, and various properties of the relaxed structure calculated, *viz.*, lattice energy, elastic constant matrix (for which the values in the principal diagonal must be positive for a structure to be stable against distortion), piezoelectric stress and strain matrices, low and high frequency relative permittivity tensors, and phonon spectra (for which frequencies must be non-negative for a stable structure). In all cases described (except where otherwise mentioned below), the structures were stable to distortion. (The lowest frequency was sometimes reported as -0.05 cm^{-1} , or less, but this is ascribed to numerical inaccuracy in the calculations rather than to structural instability.)

Results

Modelling of the room-temperature structure of KTP¹⁰ proved unusually straightforward, use of the ionic potentials and their parameters described above led directly, *via* a ‘fit relax’ cycle, to a successful description of the structure. Similarly, it proved easy to generate successful descriptions of other structures isomorphous with KTP, namely KTA,^{19,20} KSP,¹⁰ TTP,^{11,21} RTP,^{22,23} KVP,^{24,25} RTA³ and CTA.²⁶ This experience suggests that extension to yet other isomorphous materials is likely to be successful, given a good reference structure and using the ‘fit relax’ and (where necessary, because of disorder) the fractional site occupancy^{21,27} options of GULP. The experimental and relaxed lattice constants and fractional coordinates for KTP, TTP, RTP, KSP, KVP, KTA, RTA and CTA at ambient pressure are reported in Supplementary Tables 5–12.[§]

Pressure effects

Using the GULP code, we may simulate application of pressure (negative as well as positive) to a structure; this operates by adding the pressure–volume energy requirement, resulting from the imposition of pressure, to the crystal lattice energy. Thus, a series of relaxation (‘optimise’) calculations were performed on the structures of all eight of the materials modelled; the results are shown in Fig. 3–5, together with the corresponding experimentally observed values. Fig. 3 shows the calculated cell volumes *vs.* pressure for all eight of these materials, based on using only the ambient pressure structures as observables,

[§] The experimental and relaxed lattice constants and fractional coordinates for KTP, TTP, RTP, KSP, KVP, KTA, RTA and CTA at ambient pressure have been deposited as Supplementary Tables 5–12. Available as supplementary material (SUP 57292; 26 pp.) deposited with the British Library. Details are available from the editorial office.

Table 2 Values of fitted parameters for Buckingham potentials between ions and O(shell);^a fitted with structures alone, and with both structures and elastic constants. Items in square brackets have been retained at their input values. $U/\text{eV} = A \exp(-r/\rho) - C/r^6$ where r = interionic distance; $U(\text{core-shell})/\text{eV} = \frac{1}{2}k_s r^2$

	initial values ^b	KTP	TTP	RTP	KSP	KVP	KTA	RTA	CTA
fitted with structure alone:									
A^+ (radius/Å):		$K^+(1.38)$	$Tl^+(0.88)$	$Rb^+(1.49)$	$K^+(1.38)$	$K^+(1.38)$	$K^+(1.38)$	$Rb^+(1.49)$	$Cs^+(1.70)$
$A^-: A$	3587.57	18 889.854	4247.105	27 256.841	12 019.969	3540.354	16 102.372	17 047.137	16 947.184
ρ	0.30	0.23818	0.258335	0.246587	0.246119	0.279658	0.245824	0.260822	0.275450
Ti/Sn/V: A	186 838.42	180 939.111	180 305.487	165 020.443	2393.5584	131 773.82	191 874.49	177 552.064	172 709.49
ρ	0.16117	0.176279	0.177688	0.172683	0.313356	0.181226	0.168536	0.169998	0.172363
P/As: A	877.34	[877.34]	[877.34]	913.774	[877.34]	880.210	878.062	891.447	821.047
ρ	0.3594	[0.3594]	[0.3594]	0.367463	[0.3594]	0.361864	0.393633	0.389939	0.393993
fitted with both structure and elastic constants:									
$A^-: A$	3587.57	18 853.057	4256.138	19 997.426					
ρ	0.30	0.220121	0.257447	0.219753					
Ti/Sn: A	186 838.42	180 818.82	180 939.11	187 061.68					
ρ	0.16117	0.179674	0.176279	0.180278					
P/As: A	877.34	878.473	[877.34]	[877.34]					
ρ	0.3594	0.359401	[0.3594]	[0.3594]					

^aParameters for O(shell)–O(shell) interactions: $A = 22\,764.0$; $\rho = 0.149$; $C = 27.879$; $k_s = 74.92$; $q(\text{shell}) = -2.86902$ and $q(\text{core}) = 0.86902$. ^bSee text for sources. ^cRef. 28.

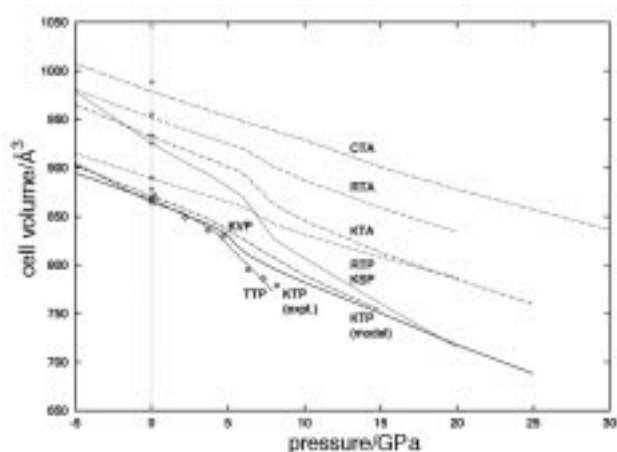


Fig. 3 Unit cell volume as a function of pressure for KTP, TTP, RTP, KSP, KVP, KTA, RTA and CTA, each modelled by fitting to their ambient pressure structures alone. The experimental ambient pressure volumes for each of the materials is also shown (by a + symbol for all except KTP, in each case closest to the respective modelled curve), as well as the experimental cell volumes of KTP (◇ symbols, without connecting lines) as a function of pressure.

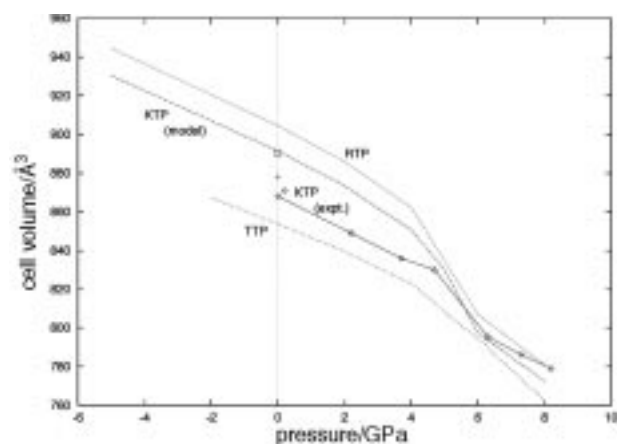


Fig. 4 Unit cell volume as a function of pressure for KTP, TTP and RTP, each modelled by fitting to both their ambient pressure structures and experimental elastic constants. The experimental ambient pressure volumes is also shown (□ for RTP; + for TTP), as well as the experimental cell volumes of KTP (◇ symbols, with connecting lines) as a function of pressure.

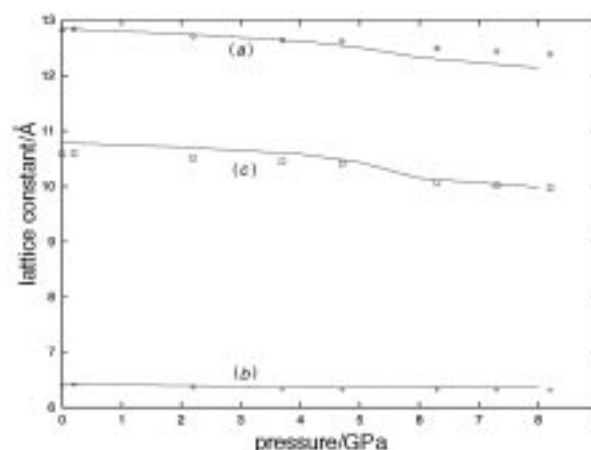


Fig. 5 Lattice constants (a , b , c) as a function of pressure for the orthorhombic cell of KTP, comparing the values from experiment (data points indicated) and modelling (lines only)

compared with the corresponding experimental data for KTP. Fig. 4 shows a second set of results for KTP, RTP and TTP, now with the fitting performed with reference to both the ambient pressure structures and the elastic constants of the materials. Fig. 5 is a plot of the individual lattice constants of KTP, comparing the modelled constants obtained by reference to the ambient pressure structure and the elastic constants with their experimental values.

It is seen in Fig. 3 that there is an excellent fit to each of the ambient pressure volumes, and that all of the cell volumes (except for CTA) follow the general trend for the KTP experimental data, albeit with a less steep volume–pressure slope for the KTP model than for the experiment. Fig. 4 shows that the fit to this slope is improved by including the experimental elastic constants in the fitting procedure, at the expense of a slightly poorer fit to the ambient pressure volumes, while Fig. 5 demonstrates that the lattice constants are individually exceedingly well described. These figures show that, experimentally, KTP undergoes a discontinuous change in unit cell volume (and of the a and c lattice constants) at *ca.* 5.8 GPa, resulting from the isosymmetric phase change. It is notable that a pressure-induced isosymmetric phase change, similar to that in KTP, has also been reported in TTP at about 6 GPa, based on observation of Raman peaks;⁹ no high-pressure experimental results are available for the other materials modelled.

Quite remarkably, the model shows essentially the same

behaviour as observed experimentally for KTP for each of the structures modelled (except, possibly, for CTA), with related changes in cell volume and in lattice constants, and each also at about 6 GPa (since we here deal with a continuous model, the modelled transition does not exhibit a clear discontinuity). An interesting observation is that the incipient phase change at a pressure of about 6 GPa is 'announced' in the relaxation calculations by a sharp increase in the number of cycles required for completion of the optimisation; this corresponds to the energy hypersurface having a long valley in this region.

The frameworks of the ambient and high-pressure structures of KTP from the modelling (Fig. 6 and 7) are essentially indistinguishable from those in the corresponding diagrams for the experimental structures (Fig. 1 and 2), while the K^+ ions are shifted (by about 0.5 Å) from their experimental positions. However, it is of considerable interest to note that the high-pressure structure which is generated (for KTP and TTP, but not for RTP) is actually rotated about the [100] direction by a two-fold axis relative to its ambient pressure progenitor structure (although this is not shown in Fig. 7, which has rather been set up to show the similarities with the experimental high-pressure structure in Fig. 2). This rotation is significant because it relates to the proposed twinning mechanism in KTP,¹² and distinguishes one of the two pro-

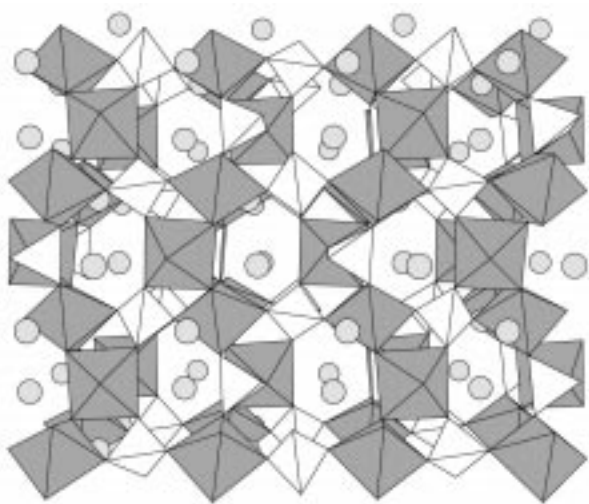


Fig. 6 Perspective view of the modelled structure of KTP at ambient pressure. The crystallographic axes are directed as in Fig. 1.

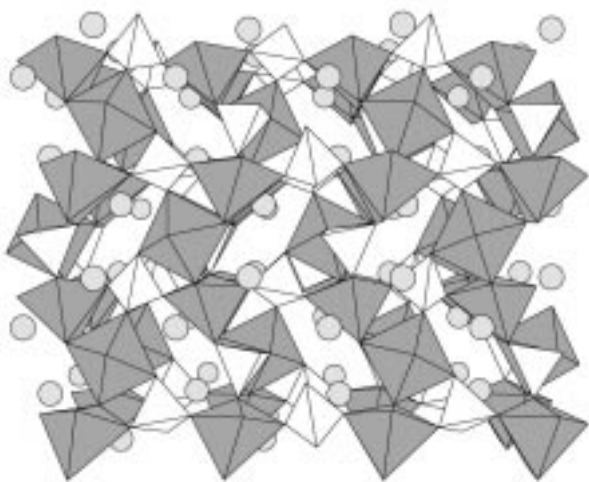


Fig. 7 Perspective view of the modelled structure of KTP at 8 GPa.⁸ The crystallographic axes have been rotated about a two-fold axis along the [100] direction relative to the axes in Fig. 1 in order to aid comparison.

posed twinning mechanisms from the other. The significance of the rotation (that is, whether there is a real transformation of this kind under pressure, or whether it is an artefact of the optimisation routine) requires further investigation.

Pressure modelling was continued to 30 GPa, well above the pressure range used in the KTP experiments (although such pressures are within the range of the diamond anvil cell, which is reported²⁸ to reach 2000 kbar or 200 GPa). Above about 8 GPa, the results become unreliable as pressure rises; for example, the cell volume for KTA continues to fall roughly linearly with pressure, until about 25 GPa, when the structure generated undergoes sudden changes in cell volume, accompanied by the appearance of negative phonon frequencies. These are clear signs that the structure is no longer stable within the imposed symmetry; such aberrant values have been omitted from Fig. 3–5.

A feature of the changes in the structures resulting from the application of pressure is that the lowest frequency A_1 transverse Raman mode connected with vibrations of the cation (experimentally, 29 cm^{-1} at 300 K for TTP, 56 cm^{-1} at 300 K for KTP; estimated—by us, by interpolation—at 43 cm^{-1} for RTP, but not available for the other materials) shows a distinct 'softening' towards lower frequency with pressure, and then a break (for TTP) or a discontinuity (for KTP) at the isosymmetric transition pressure. The calculation yields a continuous rise in frequency for this mode, although the zero-pressure frequencies correspond reasonably well with the observed values for all three materials (see Tables 3 and 4).

Temperature effects

Considerable effort was devoted to modelling the effects of temperature on these structures, but to little avail; attempts to model high-temperature structures^{9,29} and their behaviour^{30–32} led to unstable structures (see following Discussion section). Attempts were also made to allow for thermal effects in GULP, in order to better model the slope of the pressure–volume curve for KTP, but this proved to be too expensive computationally to proceed.

Discussion

The behaviour of this structural model in the study of pressure effects on the ambient structure of KTP is unprecedented in its representation of the rather uncommon isosymmetric phase change; on the other hand, such an isosymmetric phase change is peculiarly suited to modelling studies simply because the imposed symmetry restrictions need not be altered over the pressure range involved, while the accuracy of the modelling is enhanced by the many independent observations (symmetry-undetermined fractional coordinates) that these complex structures provide, together with the excellent crystal structure determinations. The elastic constants obtained are in relatively good agreement with the experimental observations¹⁸ (see Table 4); when observed values of these elastic constants are not imposed in the fitting process, then the calculated constants are a factor of about two too large.

In common with the detailed analysis in the literature^{8,10} of the experimentally observed structures, we conclude that the structures adjust to applied pressure by buckling of the framework of relatively rigid MO_6 octahedra and XO_4 tetrahedra around the A^+ ions (*cf.* Fig. 1 and 2), which is a commonly observed pattern of behaviour for frameworks involving oxygen polyhedra. However, that this is not an inevitable result is shown by the apparent lack of an isosymmetric phase change in CTA (Fig. 3); we ascribe this to the presence of the large Cs^+ ion (radius: 1.70 Å) which will support the framework.

The difficulty in modelling the high-temperature phases is possibly ascribable to disorder in the cation (A^+) positions in

Table 3 Ambient pressure properties: model with only structures of space group $Pna2_1$ fitted^a

	KTP		TTP		RTP		KSP		KVP		KTA		RTA		CTA	
	expt. ¹⁰	model	expt. ²¹	model	expt. ³	model	expt. ¹⁰	model	expt. ²⁴	model	expt. ¹⁹	model	expt. ³	model	expt. ²⁶	model
$-U_L$	31850	31794		31257		31158		31633		30334		30021		30020		30020
$a/\text{\AA}$	12.778	12.789	12.906	12.976	12.974	13.120	13.145	12.795	12.816	13.133	13.138	13.273	13.264	13.486	13.480	13.480
$b/\text{\AA}$	6.376	6.367	6.468	6.483	6.494	6.569	6.526	6.396	6.388	6.569	6.582	6.650	6.682	6.816	6.742	6.742
$c/\text{\AA}$	10.646	10.613	10.519	10.569	10.564	10.738	10.738	10.643	10.556	10.805	10.787	10.779	10.7697	10.688	10.771	10.771
V	867.31	864.15	878.08	889.08	890.05	925.38	921.15	870.92	864.21	932.09	932.80	951.46	954.52	989.02	978.81	978.81
f_{low}	56	18.1	29	60.7	(43) ^b	43		55.3		49.2		45.9		14.9		14.9

^aLattice energy $U_L/\text{kJ mol}^{-1}$; unit cell lengths $a, b, c/\text{\AA}$; unit cell volume $V/\text{\AA}^3$; lowest non-zero phonon frequency $f_{\text{low}}/\text{cm}^{-1}$. ^bInterpolated value.

Table 4 Ambient pressure properties: model with structures plus elastic constants fitted

	KTP		TTP		RTP	
	expt. ¹⁰	model	expt. ²¹	model	expt. ³	model
$-U_L$		31657		32031		31931
$a/\text{\AA}$	12.819	12.843	12.906	12.671	12.974	12.903
$b/\text{\AA}$	6.399	6.435	6.468	6.349	6.494	6.464
$c/\text{\AA}$	10.584	10.787	10.519	10.612	10.564	10.845
$V/\text{\AA}^3$	868.19	891.48	878.08	853.71	890.05	904.55
$f_{\text{low}}/\text{cm}^{-1}$	56	37	29	24	43 ^a	26
C_{11}/GPa	166	253	156	276	163	250
C_{22}/GPa	164	252	154	276	165	248
C_{33}/GPa	181	221	166	269	178	210
C_{44}/GPa	56	69	45	77	58	67
C_{55}/GPa	54	76	49	83	57	74
C_{66}/GPa	45	30	49	36	50	29
C_{12}/GPa	37	23	40	32	45	23
C_{13}/GPa	54	52	49	60	35	51
C_{23}/GPa	51	36	63	28	70	34

^aInterpolated value.

the paraelectric phase, as noted by Harrison *et al.*,¹¹ by Favard *et al.*³³ and in much detail for the germanate structures by Belokoneva *et al.*³⁴

Taking the results as a whole, there has been a successful modelling of structures within the KTP system in the low temperature (ferroelectric) phase and the problems associated with modelling the high-temperature phase are understood. It should be readily possible to extend the modelling, using the same techniques, to other isomorphous materials and to the mixed systems whose structural properties are of considerable scientific and technological interest.

Note added in proof. After acceptance of this manuscript, it has been reported³⁵ by Raman spectroscopy that KTA undergoes three phase transitions under pressure, the first (at 3.2 GPa) being similar to that predicted in this paper.

L. Glasser acknowledges the support of the University of the Witwatersrand and the South African FRD for sabbatical leave in the UK, and the provision of facilities by the Chemical Crystallography group at Oxford University. Particular thanks are offered to Dr J. D. Gale for his support of the work with GULP, and to Dr Pamela Thomas (Warwick) and Dr David Allan (Edinburgh) for discussions.

Access to the Inorganic Crystal Structure Database (ICSD) was of considerable assistance in locating structural information, and is much appreciated.

References

- G. D. Stucky, M. L. F. Phillips and T. E. Gier, *Chem. Mater.*, 1989, **1**, 492; M. E. Hagerman and K. R. Poeppelmeier, *Chem. Mater.*, 1995, **7**, 602.
- V. K. Yanovskii and V. I. Voronkova, *Phys. Status Solidi A*, 1986, **93**, 655.
- P. A. Thomas, S. C. Mayo and B. E. Watts, *Acta Crystallogr., Sect. B*, 1992, **48**, 401.
- G. A. Kourouklis, A. Jayaraman and A. A. Ballman, *Solid State Commun.*, 1987, **62**, 379.
- D. R. Allan, J. S. Loveday, R. J. Nelmes and P. A. Thomas, *Ferroelectrics*, 1991, **124**, 367.
- D. R. Allan and R. J. Nelmes, *J. Phys.: Condens. Matter*, 1992, **4**, L395.
- D. R. Allan, J. S. Loveday, R. J. Nelmes and P. A. Thomas, *J. Phys.: Condens. Matter*, 1992, **4**, 2747.
- D. R. Allan and R. J. Nelmes, *J. Phys.: Condens. Matter*, 1996, **8**, 2337; 5951.
- M. Serhane, C. Dugautier, R. Farhi, P. Moch and R. V. Pisarev, *Ferroelectrics*, 1991, **124**, 373.
- P. A. Thomas, A. M. Glazer and B. E. Watts, *Acta Crystallogr.*,

- Sect. B, 1990, **46**, 333; See also M. L. F. Phillips, W. T. A. Harrison and G. D. Stucky, *Inorg. Chem.*, 1990, **29**, 3245.
- 11 W. T. A. Harrison, T. E. Gier, G. D. Stucky and A. J. Schultz, *Mater. Res. Bull.*, 1995, **30**, 1341.
 - 12 P. A. Thomas, I. J. Tebbutt and A. M. Glazer, *J. Appl. Crystallogr.*, 1991, **24**, 963; P. A. Thomas and A. M. Glazer, *J. Appl. Crystallogr.*, 1991, **24**, 968.
 - 13 J. D. Gale, GULP—General Utility Lattice Program, Imperial College/Royal Institution of Great Britain, version 1.0, 1996; J. D. Gale, *J. Chem. Soc., Faraday Trans.*, 1997, **93**, 629.
 - 14 C. R. A. Catlow and R. James, *Proc. R. Soc. London, Ser. A*, 1982, **384**, 157; C. R. A. Catlow, C. M. Freeman, S. M. Tomlinson, M. S. Islam, R. A. Jackson and M. Leslie, *Philos. Mag. A*, 1988, **58**, 123.
 - 15 J. D. Gale and N. J. Henson, *J. Chem. Soc., Faraday Trans.*, 1994, **90**, 3175.
 - 16 T. S. Bush, J. D. Gale, C. R. A. Catlow and P. D. Battle, *J. Mater. Chem.*, 1994, **4**, 831.
 - 17 H. le Roux and L. Glasser, *J. Mater. Chem.*, 1997, **7**, 843.
 - 18 M. Serhane and P. Moch, *J. Phys.: Condens. Matter*, 1994, **6**, 3821.
 - 19 S. C. Mayo, P. A. Thomas, S. J. Teat, G. M. Loiacono and D. N. Loiacono, *Acta Crystallogr., Sect. B*, 1994, **50**, 655.
 - 20 P. A. Northrup, J. B. Parise, L. K. Cheng, L. T. Cheng and E. M. McCarron, *Chem. Mater.*, 1994, **6**, 434.
 - 21 N. I. Sorokina, V. I. Voronkova, V. K. Yanovskii, D. Y. Lee, M. Jannin, C. Kolinsky, G. Godefroy, B. Jannot and V. I. Simonov, *Crystallogr. Rep.*, 1997, **42**, 39 (transl. from *Kristallografiya*, 1997, **42**, 47); D. Y. Lee, N. I. Sorokina, V. I. Voronkova, V. K. Yanovskii, I. A. Verin and V. I. Simonov, *Crystallogr. Rep.*, 1997, **42**, 218 (transl. from *Kristallografiya*, 1997, **42**, 255).
 - 22 J. A. Kaduk and R. H. Jarman, *Z. Kristallogr.*, 1993, **204**, 285.
 - 23 A. S. Lyakhov, A. F. Selevich and A. I. Verenich, *Russ. J. Inorg. Chem.*, 1993, **38**, 1040 (transl. from *Zh. Neorg. Khim.*, 1993, **38**, 1121).
 - 24 M. L. F. Phillips, W. T. A. Harrison, T. E. Gier, G. D. Stucky, G. V. Kulkarni and J. K. Burdett, *Inorg. Chem.*, 1990, **29**, 2158.
 - 25 L. Benhamada, A. Grandin, M. M. Borel, A. Leclaire and B. Raveau, *Acta Crystallogr., Sect. C*, 1991, **47**, 1138. [Note: this structure for KVP did not yield a successful modelling: the crystals are described as 'dark blue', whereas ref. 24 above (also for KVP) yields a successful modelling, and describes the material as either 'dark orange crystals' or 'a dark brown powder'.]
 - 26 J. Protas, G. Marnier, B. Boulanger and B. Menaert, *Acta Crystallogr., Sect. C*, 1989, **45**, 1123.
 - 27 P. A. Thomas, R. Duhlev and S. J. Teat, *Acta Crystallogr., Sect. B*, 1994, **50**, 538.
 - 28 P. W. Atkins, *Physical Chemistry*, 5th edn., Oxford University Press, Oxford, 1994.
 - 29 W. T. A. Harrison, T. E. Gier, G. D. Stucky and A. J. Schultz, *J. Chem. Soc., Chem. Commun.*, 1990, 540.
 - 30 R. V. Pisarev, R. Farhi, P. Moch and V. I. Voronkova, *J. Phys.: Condens. Matter*, 1990, **2**, 7555.
 - 31 R. Farhi, P. Moch and R. V. Pisarev, *Phase Transitions*, 1991, **33**, 65.
 - 32 V. I. Voronkova, V. K. Yanovskii, N. I. Sorokina, I. A. Verin and V. I. Simonov, *Crystallogr. Rep.*, 1993, **38**, 66 (transl. from *Kristallografiya*, 1993, **38**, 147).
 - 33 J.-F. Favard, A. Verbaere, Y. Piffard and M. Tournoux, *Eur. J. Solid State Inorg. Chem.*, 1994, **31**, 995.
 - 34 E. L. Belokoneva, K. S. Knight, W. I. F. David and B. V. Mill', *J. Phys.: Condens. Matter*, 1997, **9**, 3833.
 - 35 Z. X. Shen, X. B. Wang, H. P. Li, S. H. Tang and F. Zhou, *Rev. High Press. Sci Technol.*, 1997, in press.

Paper 7/04337F; Received 20th June, 1997